Identification of Key Genes and Pathways associated with Chemotherapy and Radiotherapy Sensitivity in Locally Advanced Cervical Cancer

Zhenhua Zhang
The Affiliated Hospital of Southwest Medical University
Yao Zhang
Southwest Medical University
Yongshun Ma
Southwest Medical University
Shixing Xiang
Southwest Medical University
Jing Shen
Southwest Medical University
Yueshui Zhao
Southwest Medical University
Xu Wu
Southwest Medical University
Mingxing Li
Southwest Medical University
Xiao Yang
Southwest Medical University
Parham Jabbarzadeh Kaboli
Southwest Medical University
Fukuan Du
Southwest Medical University
Huijiao Ji
Southwest Medical University
Lin Liu
The Affiliated Stomatology Hospital of Southwest Medical University
Zhangang Xiao (✉ zhangangxiao@swmu.edu.cn)
Southwest Medical University https://orcid.org/0000-0003-4265-5833
Jing Li
The Affiliated Hospital of Southwest Medical University
Qinglian Wen

The Affiliated Hospital of Southwest Medical University

Primary research

Keywords: locally advanced cervical cancer, radiotherapy and chemotherapy, responders and non-responders, microarray, differentially expressed gene, single cell sequence

Posted Date: December 4th, 2020

DOI: https://doi.org/10.21203/rs.3.rs-120262/v1

Abstract

Objectives Currently, the standard treatment approach for locally advanced cervical cancer (LACC) is concurrent chemoradiotherapy (CCRT). However, resistance to radiotherapy and chemotherapy often leads to treatment failure. Intrinsic resistance is often a decisive factor in treatment response. Thus, it is urgent to identify the key genes and pathways associated with CCRT sensitivity in LACC.

Materials and Methods We searched the Gene Expression Omnibus (GEO) database for patients with LACC and analyzed differentially expressed genes (DEGs) between responders and non-responders. Gene Ontology (GO) enrichment analysis of DEGs were performed using DAVID tools. And Kyoto Encyclopedia of Genes and Genomes (KEGG) pathway enrichment analysis of DEGs were conducted using R package cluster Profiler. The Weighted Gene Co-Expression Network Analysis (WGCNA) from R package WGCNA was used for the identification of highly correlated gene modules. A protein-protein interaction (PPI) network was constructed using STRING and 20 hub genes were selected. The expression levels of these 20 genes were was analyzed using The Cancer Genome Atlas (TCGA) and Gene Expression Profiling Interactive Analysis (GEPIA 2) databases. Furthermore, single-cell transcriptome sequencing was used to elucidate the cell type composition of the cervix sample and analyze the expression levels of 10 hub genes in cells.

Results: Compared with non-responders, 580 genes were significantly up-regulated. The up-regulated genes were mainly related to Human papillomavirus infection, focal adhesion, and ECM-receptor interaction signaling pathway. We screened 10 hub genes (COL1A1, COL6A1, COL6A2, LAMA4, COL6A3, LAMC1, HSPG2, ITGA9, CTGF, PDGFRB) and further studied them. Compared with healthy people, these 10 genes were low expressed in cervical cancer patients, and their mRNA levels were positively correlated. Receiver Operator Characteristic curve (ROC) analysis indicated that 10 hub genes could differentiate responders from non-responders. Furthermore, we showed that COL1A1, COL6A1, COL6A2 were highly expressed after radiotherapy or chemoradiotherapy. By analyzing the single-cell sequence, we found that the main cell types in cervical tissue include Fibroblasts, Smooth muscle cells, Tissue stem cells, Endothelial cells, Progenitor cells, Epithelial cells, T cells, Basal cells, Macrophages, and Mast cells. And COL1A1, COL6A1, COL6A2, COL6A3, CTGF, PDGFRB were highly expressed in Progenitor cells.

Conclusions: In summary, COL1A1, COL6A1, COL6A2, LAMA4, COL6A3, LAMC1, HSPG2, ITGA9, CTGF, and PDGFRB might serve as therapeutic targets to enhance the therapeutic effect of CCRT in the treatment of LACC. These genes were involved in Human papillomavirus infection, focal adhesion, and ECM-receptor interaction signaling pathway. And they were involved in various biological processes, including cell adhesion and extracellular matrix organizations. Besides, COL1A1, COL6A1, COL6A2, COL6A3, CTGF, and PDGFRB were highly expressed in Progenitor cells.

Introduction

Cervical cancer is one of the leading causes of cancer death among women worldwide. The treatment of cervical cancer remains a major therapeutic challenge for researchers and physicians [1]. Moreover, morbidity and mortality in developing countries are significantly increased compared with developed countries [2–4]. There are two types of cervical cancer, squamous cell carcinoma (SCC) and adenocarcinoma (AC), of which SCC accounts for the largest proportion [5, 6]. One report from a developing country has shown that over 80% of new cervical cancer cases are found at advanced stages [7]. At present, the treatment of LACC mainly includes operation, chemotherapy, radiotherapy, or combined treatment [8–10]. CCRT based on cisplatin is the primary treatment for LACC (patients with stage □B2-□A), CCRT was reported improved overall survival and progression-free survival in LACC [11–13]. Cisplatin is used to treat a variety of cancers, It interferes with the DNA repair mechanism, causes DNA damage, induces apoptosis of cancer cells [14]. However, in the past work, we have found that treatment resistance for some patients with LACC [15–17]. For patients who do not respond to CCRT, other effective treatment options need to be adopted. Therefore, we need to look for genes and signaling pathways associated with the treatment of LACC.

In the present study, we explored the interaction network of differentially expressed genes (DEGs) between responders and non-responders along with interrelated signaling pathways in LACC by analyzing the expression profile of gene expression microarray data (GSE56303-GPL10191, GSE56303-GPL16025, and GSE56363) using bioinformatics tools. The purpose of this study is to find more CCRT sensitivity-related key genes and pathways, which might serve as targets to increase CCRT sensitivity. And the expression of these genes in cervical tissue cells was analyzed. We attempt to elucidate the causes of failure of radiotherapy and chemotherapy for locally advanced cervical cancer.

Materials And Methods

Data acquisition

Microarray gene expression profiles were obtained from a previous study published in the GEO database [18] (GEO Accession number GSE56303 [19]; https://www.ncbi.nlm.nih.gov/geo/query/acc.cgi?acc=GSE56303 and GEO Accession number GSE56363 [20]; https://www.ncbi.nlm.nih.gov/geo/query/acc.cgi?acc=GSE56363). The keyword of the search is " locally advanced cervical cancer ". The restricted research type is expression profiling by array, and the restricted species is Homo sapiens. The selected data meets the following criteria: (1) The data set must be the expression mRNA chip data of the whole cervical cancer genome; (2) The data must be a controlled study of the effectiveness and inefficacy of CCRT for LACC; (3) The data set case (responders) - control (non-responders) group must include or exceed 3 Samples; (4) Information on treatment results for each sample must be provided. Data sets meeting the above criteria will be included in this study. Finally, there are two datasets of data that meet our standards: GSE56303 (platform: GPL10191 NimbleGen Homo sapiens HG18 090828 opt expr HX12 (12x135k); GPL16025 NimbleGen Homo sapiens Expression Array [100718_HG18_opt_expr]) and GSE6363 (platform: GPL4133 Agilent-014850 Whole Human Genome Microarray 4x44K G4112F (Feature Number version)). The GSE56303 dataset contains gene expression

profiles of 63 responders defined as the disappearance of all signs of cancer in response to treatment and 22 non-responder patients (defined as patients with partial, progressive, or stable disease), patients with a confirmed pathologic diagnosis of CC staged IB2 up to IIIB. The GSE56363 dataset contains 21 patients with locally advanced squamous cell carcinoma (FIGO stage IIB-IIIB): 12 responders and 9 non-responder patients **(Table 1)**.

Identification of DEGs in responders and non-responders

Limma R package [21] was used to identify the DEGs between responders and non-responders through R software (version 3.5.2; https://cran.r-project.org/). Fold-change (FC) values were calculated and the DEGs were further selected based on the following cutoff criteria: $P<0.05$ and the absolute value of $\log_2$ FC (fold change) >0.5. The intersecting DEGs of responders and non-responders were used for further analysis.

Gene ontology and pathway enrichment analysis

To identify the enriched function of 580 up-regulated DEGs, we used the DAVID online tool [22] to perform GO analyses. GO analysis including three independent categories: biological process (BP), cellular component (CC), and molecular function (MF). KEGG pathway enrichment analysis of DEGs were conducted using the clusterProfiler package [23]. Adjusted pvalue < 0.05 as the threshold level for statistical significance.

Identification of genes associated with clinical characteristics

In this study, all genes were involved to perform the WGCNA analysis by the R package WGCNA [24]. WGCNA uses the topological overlap measure (TOM) as a proximity measure to cluster genes into network modules that combine the adjacency of two genes and the connection strengths with which these two genes interact with other neighbor genes. A soft thresholding parameter was employed to construct a weighted network. Here, we constructed co-expression modules through WGCNA related to clinical traits, and obtained genes associated with clinical traits through WGCNA.

PPI network construction and hub genes identification

We used the STRING [25] to search the potential interactions between known proteins and predicted proteins. It is the largest database for protein interaction information at present. Through this database, we construct a PPI network, which was visualized using Cytoscape (version 3.7.1) [26]. And 20 hub genes were selected from the PPI network using the MCC algorithm of the CytoHubba plugin [27].

Expression analysis of 20 hub genes

The Gene Expression Profiling Interactive Analysis (GEPIA 2, http://gepia2.cancer-pku.cn/) webserver has been a valuable and highly cited resource for gene expression analysis based on tumor and normal samples. To compare the difference in gene expression between cervical cancer patients and healthy

people, we used GEPIA 2 [28] for analysis. The Cancer Genome Atlas (TCGA, https://cancergenome.nih.gov/) database is a publicly funded project aimed at classifying and discovering major genomic changes in cancer to create a comprehensive cancer genome map. In this study, Gene expression data of cervical cancer patients were obtained from the TCGA database and co-expression analysis was performed. The correlation of mRNA expression was analyzed by the Pearson test. P<0.05 was considered to indicate statistically significant differences.

Further analysis of 10 down-regulated genes in cancer.

Receiver operating characteristic (ROC) curve analysis was performed to assess the diagnostic performance in characterizing responders versus non-responders and determine the area under the ROC curve(AUC). To compare the difference of gene expression before and after chemoradiotherapy, we searched the public database GEO database (GSE3578 [29]; https://www.ncbi.nlm.nih.gov/geo/query/acc.cgi?acc=GSE3578).

Single-cell sequence analysis of a cervical tissue

We performed a single-cell transcriptome sequencing analysis of a cervical sample (GSM3980130 [30]; https://www.ncbi.nlm.nih.gov/geo/query/acc.cgi?acc=GSM3980130). The Seurat package [31] in R 4.0.0 was used for quality control, statistical analysis, and exploration of the scRNA-seq data. The sample contained 10,000 cells, and after quality control, a total of 9955 cells were included in this analysis. Then, the gene expression of the remaining 9955 cells was normalized using a linear regression model. PCA was performed to identify significantly available dimensions with a P-value < 0.05 [32]. Then, the uniform manifold approximation and projection (UMAP) [33] algorithm was applied for dimensionality reduction with 20 PCs and for performing cluster classification analysis. The differential expression analysis among all genes within cell clusters was performed to identify the marker genes of each cluster. Afterward, different cell clusters were determined and annotated by the singleR [34] package according to the marker genes and were then manually verified and corrected with the CellMarker [35] database and PanglaoDB [36]. The cell marker genes used for cluster annotation are shown in **Supplementary Table 5**. Here, we elucidated the cell type composition of the cervix sample by scRNA-seq sequence analysis and analyze the expression levels of 10 hub genes in cells.

Results

The DEGs between the response group and the non-response group were identified.

The limma package was used to estimate the fold changes and standard errors by fitting a linear model for each gene for the assessment of differential expression. As shown in Fig. 1a. We set the cut-off criteria as p-value < 0.05 and $|\log_2 FC| > 0.5$ to screen the DEGs. There were 1358 significant differential genes in GSE56303-GPL10191, including 860 up-regulated genes and 498 down-regulated genes. There are 6048 differential genes in GSE56303-GPL16025, among which 3204 are up-regulated genes and 2844 are down-regulated. There are 4214 differentially expressed genes in GSE56363, including 2133 up-

regulated genes and 2081 down-regulated genes (**Supplementary Table 1**). In summary, 580 up-regulated genes and 153 down-regulated genes represent the differentially regulated genes in two or more datasets (Fig. 1b).

Up-regulated DEGs were enriched to key functions and pathways.

Go and KEGG analysis revealed that 153 down-regulated genes were not enriched in meaningful functions and pathways. The GO analysis of the 580 up-regulated DEGs was mainly enriched for the BP terms cell adhesion and extracellular matrix organization. GO analysis in the category CC showed that the DEGs were mainly accumulated in the extracellular matrix, extracellular exosome, membrane. The MF of the DEGs were mainly related to protein binding and calcium ion binding (Fig. 2a). Additionally, Up-regulated DEGs were significantly associated with Human papillomavirus infection **(Supplementary Fig. 1)**, Focal adhesion, Lysosome, Hippo signaling pathway, Protein processing in endoplasmic reticulum, and ECM-receptor interaction signaling pathway (Fig. 2b). We showed the correlation between genes and pathways (Fig. 2c **& Supplementary Table 2)**. Furthermore, we analyzed the correlation between pathways and pathways, and we found that Human papillomavirus infection, Focal adhesion and ECM-receptor interaction signaling pathway were correlated (Fig. 2d).

Identification of genes associated with clinical features based on WGCNA

We have chosen the soft threshold power 6 to define the adjacency matrix based on the criterion of approximate scale-free topology **(Supplementary Fig. 2)**. The network and the 4 identified modules are depicted in Fig. 3a, b. Figure 3c provides an alternate visualization of the module structure via a multi-dimensional scaling plot (standard R function cmdscale). Furthermore, we performed cluster analysis, Fig. 3d depicts the eigengene network using a dendrogram (hierarchical cluster tree). In general, 4 clusters were grouped into two clusters, the blue and grey modules are highly correlated. Combined with Fig. 3e, the blue modules were related to therapeutic effect.

Ten Hub Genes Are Associated With Chemoradiotherapy

Through ROC curve analysis, we found that COL1A1, COL6A1, COL6A2, LAMA4, COL6A3, LAMC1, HSPG2, ITGA9, CTGF, and PDGFRB had better diagnostic performance in distinguishing responders from non-responders in datasets of GSE56303-GPL16025 and GSE56363. The AUC values of these genes were all greater than 0.7 in GSE56303-GPL16025 and GSE56363 (Fig. 5a). More importantly, the expression levels of COL1A1, COL6A1, COL6A2 were significantly increased in cervical cancer patients after radiotherapy or chemoradiotherapy (Fig. 5b).

Six hub genes were highly expressed in the Progenitor cells of cervical tissue

The sample contained 10,000 cells, the filtering parameters were set to nFeature_RNA > 200 & nFeature_RNA < 2000 &Percent.mt < 40 & nCount_RNA < 4000, and 9955 cells were included in the analysis **(Supplementary Fig. 3a)**. We selected 20 principal components (PCs) with an estimated P_value

< 0.05 for subsequent analysis **(Supplementary Fig. 3b)**. Afterward, the uniform manifold approximation and projection (UMAP) algorithm was applied, and cells in the cervix were successfully classified into 12 separate clusters **(**Fig. 6a**)**. We show the expression levels of the top 5 marker genes in each cluster with a heat map **(Supplementary Fig. 3c)**. According to the expression patterns of the marker genes, these clusters were annotated by singleR, CellMarker, and PanglaoDB **(**Fig. 6b**)**. Cluster 0, 3, and 4, containing 4126 cells, were annotated as Fibroblasts; clusters 1 and 2, containing 3215, were annotated as Smooth muscle cells; cluster 5, containing 657 cells, was annotated as Tissue stem cells; cluster 6, containing 521 cells, was annotated as Endothelial cells; cluster 7, containing 485 cells, was annotated as Progenitor cells; cluster 8, containing 389 cells, was annotated as Epithelial cells; cluster 9, containing 217 cells, was annotated as T cells; cluster 10, containing 182 cells, was annotated as Basal cells; cluster 11, containing 116 cells, was annotated as Macrophages; cluster 12, containing 47 cells, was annotated as Mast cells. We analyzed the expression of 10 hub genes in cervical sample cells, and the results showed that COL1A1, COL6A1, COL6A2, COL6A3, CTGF, and PDGFRB were highly expressed in progenitor cells (cluster 7) **(**Fig. 6c**)**.

Discussion

Cervical cancer remains a major health problem for women in developing countries. Cervical cancer is deadly because most patients are already advanced at the time of diagnosis [37, 38]. About half of patients with LACC will relapse or metastasize within the first two years after treatment, up to 40% of patients have no response to conventional treatment [39]. The treatment of LACC is a complex biological process. In recent years, although many new treatment methods have emerged, CCRT is still the main treatment method [12, 40]. The reasons for the ineffectiveness of CCRT in the treatment of LACC are not fully understood, and studies at the signaling pathways may help to explain this phenomenon. In this study, we have integrated the data of responders and non-responders to radiotherapy and chemotherapy for LACC, 10 hub genes (COL1A1, COL6A1, COL6A2, LAMA4, COL6A3, LAMC1, HSPG2, ITGA9, CTGF, and PDGFRB) were identified by analyzing LACC patients with CCRT sensitivity, the expression levels of these genes in cervical cancer were decreased and correlated positively with each other. COL1A1, COL6A1, COL6A2, LAMA4, COL6A3, LAMC1, HSPG2, ITGA9, CTGF, and PDGFRB were mainly enriched in the Human papillomavirus infection, focal adhesion, and ECM-receptor interaction signaling pathway. In addition, we also discussed the cell types of cervical samples and the expression levels of these 10 genes in the cells indicated that COL1A1, COL6A1, COL6A2, COL6A3, CTGF, and PDGFRB were highly expressed in Progenitor cells. These studies provide further evidence to clarify the reasons for the failure of CCRT in the treatment of LACC. These results may be the basis for developing new targeted strategies to improve the prognosis of cervical cancer.

In this study, we found that the failure of chemoradiotherapy for cervical cancer was associated with Human papillomavirus infection, focal adhesion, and ECM-receptor interaction signaling pathway. Cervical cancer is the second most common cancer in women worldwide, persistent infection with one of about 15 genotypes of carcinogenic human papillomavirus (HPV) causes almost all cases, HPV has been identified as a major factor that leads to cervical cancer [9, 41, 42].

Among the myriad of microenvironmental factors impacting on cancer cell resistance, cell adhesion to the extracellular matrix (ECM) has recently been identified as a key determinant [43–45]. The extracellular matrix (ECM) drives metastasis via its interaction with the integrin signaling pathway, contributes to tumor progression, and confers therapy resistance by providing a physical barrier around the tumor [46].

In summary, our analysis found that chemoradiotherapy resistance in LACC is associated with human papillomavirus infection, focal adhesion, and ECM receptor interaction signaling pathways. And we identified hub genes that might be associated with chemoradiotherapy failure, which might be useful for the accurate diagnosis and treatment of LACC.

In order to apply the findings to the treatment of patients, we need to do more work: (i) as only two microarray profiles were analyzed, the sample size was not sufficiently large; thus, large-sample studies are required to validate the findings. (ii) In order to analyze the effect of target gene expression on the efficacy of radiotherapy and chemotherapy for advanced cervical cancer, more experiments should be encouraged to further verify our results. (iii) It is necessary to study the cell types of responders and non-responders using single-cell techniques.

Abbreviations

GEO
Gene Expression Omnibus
David
Database for Annotation, Visualization and Integrated Discovery
GO
Gene ontology
KEGG
Kyoto Encyclopedia of Genes and Genomes
CCRT
Concomitant chemotherapy and radiotherapy
DEGs
Differentially expressed genes
PPI
Protein-protein interaction
SCC
Squamous cell carcinoma
LACC
Locally advanced cervical cancer
AC
Adenocarcinoma
STRING
Search Tool for the Retrieval of Interacting Genes

TCGA
The Cancer Genome Atlas
WGCNA
Weighted Gene Co-Expression Network Analysis
ROC
Receiver operating characteristic
AUC
area under the curve

Declarations

Funding

This work was supported by National Natural Science Foundation of China (grant number: 81672444, 81972643), Sichuan Science and Technology Project (grant number: 2018JY0079), and Luxian - Southwest Medical University Strategic Cooperation Achievement Transfer and Transformation Cultivation Project (grant number: 2019LXXNYKD-07).

Data Availability Statement

The datasets analyzed during the current study are available in the TCGA (https://cancergenome.nih.gov/) and GEO (https://www.ncbi.nlm.nih.gov/geo/) databases.

Acknowledgments

The authors thank the National Natural Science Foundation of China, Sichuan Science and Technology Project, and Luxian - Southwest Medical University Strategic Cooperation Achievement Transfer and Transformation Cultivation Project for funding supporting.

Contributions

ZX, JL, and WQ supervised the project. ZZ, YZ, and YM collected the data and analyzed data. SX, JS, YZ, XW, ML, and XY wrote the manuscript and commented on the manuscript. PK, FD, HJ, and LL provided scientific expertise.

Ethics declarations

Ethics approval and consent to participate

Not applicable.

Consent for publication

Not applicable.

Competing interests

The authors declare that they have no competing interests.

Acknowledgements

Not applicable.

References

1. Bray F, Ferlay J, Soerjomataram I, Siegel RL, Torre LA, Jemal A. Global cancer statistics 2018: Globocan estimates of incidence and mortality worldwide for 36 cancers in 185 countries. Cancer J Clin. 2018;68:394–424.
2. Torre LA, Bray F, Siegel RL, Ferlay J, Lortet-Tieulent J, Jemal A. Global cancer statistics, 2012. Cancer J Clin. 2015;65:87–108.
3. Sant M, Aareleid T, Berrino F, Bielska Lasota M, Carli PM, Faivre J, Grosclaude P, Hedelin G, Matsuda T, Moller H, Moller T, Verdecchia A, Capocaccia R, Gatta G, Micheli A, Santaquilani M, Roazzi P, Lisi D, Group EW. Eurocare-3: Survival of cancer patients diagnosed 1990-94–results and commentary. Annals of oncology: official journal of the European Society for Medical Oncology. 2003;14(Suppl 5):v61–118.
4. Ferlay J, Shin HR, Bray F, Forman D, Mathers C, Parkin DM. Estimates of worldwide burden of cancer in 2008: Globocan 2008. International journal of cancer. 2010;127:2893–917.
5. Lonnberg S, Hansen BT, Haldorsen T, Campbell S, Schee K, Nygard M. Cervical cancer prevented by screening: Long-term incidence trends by morphology in norway. International journal of cancer. 2015;137:1758–64.
6. Williams NL, Werner TL, Jarboe EA, Gaffney DK. Adenocarcinoma of the cervix: Should we treat it differently? Current oncology reports. 2015;17:17.
7. Kokka F, Bryant A, Brockbank E, Powell M, Oram D. Hysterectomy with radiotherapy or chemotherapy or both for women with locally advanced cervical cancer. The Cochrane database of systematic reviews 2015:CD010260.
8. Yang PM, Chou CJ, Tseng SH, Hung CF. Bioinformatics and in vitro experimental analyses identify the selective therapeutic potential of interferon gamma and apigenin against cervical squamous cell carcinoma and adenocarcinoma. Oncotarget. 2017;8:46145–62.
9. Waggoner SE. Cervical cancer. Lancet. 2003;361:2217–25.
10. Marquina G, Manzano A, Casado A. Targeted agents in cervical cancer: Beyond bevacizumab. Current oncology reports. 2018;20:40.
11. Pearcey R, Miao Q, Kong W, Zhang-Salomons J, Mackillop WJ. Impact of adoption of chemoradiotherapy on the outcome of cervical cancer in ontario: Results of a population-based

cohort study. Journal of clinical oncology: official journal of the American Society of Clinical Oncology. 2007;25:2383–8.

12. Green J, Kirwan J, Tierney J, Vale C, Symonds P, Fresco L, Williams C, Collingwood M. Concomitant chemotherapy and radiation therapy for cancer of the uterine cervix. The Cochrane database of systematic reviews 2005:CD002225.
13. Rose PG, Bundy BN, Watkins EB, Thigpen JT, Deppe G, Maiman MA, Clarke-Pearson DL, Insalaco S. Concurrent cisplatin-based radiotherapy and chemotherapy for locally advanced cervical cancer. N Engl J Med. 1999;340:1144–53.
14. Dasari S, Tchounwou PB. Cisplatin in cancer therapy: Molecular mechanisms of action. Eur J Pharmacol. 2014;740:364–78.
15. Kumar L, Harish P, Malik PS, Khurana S. Chemotherapy and targeted therapy in the management of cervical cancer. Curr Probl Cancer. 2018;42:120–8.
16. Lippert TH, Ruoff HJ, Volm M. Intrinsic and acquired drug resistance in malignant tumors. The main reason for therapeutic failure. Arzneimittelforschung. 2008;58:261–4.
17. Zhu H, Luo H, Zhang W, Shen Z, Hu X, Zhu X. Molecular mechanisms of cisplatin resistance in cervical cancer. Drug Des Devel Ther. 2016;10:1885–95.
18. Edgar R, Domrachev M, Lash AE. Gene expression omnibus: Ncbi gene expression and hybridization array data repository. Nucleic acids research. 2002;30:207–10.
19. Fernandez-Retana J, Lasa-Gonsebatt F, Lopez-Urrutia E, Coronel-Martinez J, Cantu De Leon D, Jacobo-Herrera N, Peralta-Zaragoza O, Perez-Montiel D, Reynoso-Noveron N, Vazquez-Romo R, Perez-Plasencia C. Transcript profiling distinguishes complete treatment responders with locally advanced cervical cancer. Translational oncology. 2015;8:77–84.
20. Balacescu O, Balacescu L, Tudoran O, Todor N, Rus M, Buiga R, Susman S, Fetica B, Pop L, Maja L, Visan S, Ordeanu C, Berindan-Neagoe I, Nagy V. Gene expression profiling reveals activation of the fa/brca pathway in advanced squamous cervical cancer with intrinsic resistance and therapy failure. BMC Cancer. 2014;14:246.
21. Ritchie ME, Phipson B, Wu D, Hu Y, Law CW, Shi W, Smyth GK. Limma powers differential expression analyses for rna-sequencing and microarray studies. Nucleic acids research. 2015;43:e47.
22. Huang da W, Sherman BT, Lempicki RA. Systematic and integrative analysis of large gene lists using david bioinformatics resources. Nature protocols. 2009;4:44–57.
23. Yu G, Wang LG, Han Y, He QY. Clusterprofiler: An r package for comparing biological themes among gene clusters. Omics: a journal of integrative biology. 2012;16:284–7.
24. Langfelder P, Horvath S. Wgcna: An r package for weighted correlation network analysis. BMC Bioinform. 2008;9:559.
25. Szklarczyk D, Gable AL, Lyon D, Junge A, Wyder S, Huerta-Cepas J, Simonovic M, Doncheva NT, Morris JH, Bork P, Jensen LJ, Mering CV. String v11: Protein-protein association networks with increased coverage, supporting functional discovery in genome-wide experimental datasets. Nucleic acids research. 2019;47:D607–13.

26. Doncheva NT, Morris JH, Gorodkin J, Jensen LJ. Cytoscape stringapp: Network analysis and visualization of proteomics data. J Proteome Res. 2019;18:623–32.
27. Bader GD, Hogue CW. An automated method for finding molecular complexes in large protein interaction networks. BMC Bioinform. 2003;4:2.
28. Tang Z, Kang B, Li C, Chen T, Zhang Z. Gepia2: An enhanced web server for large-scale expression profiling and interactive analysis. Nucleic acids research. 2019;47:W556–60.
29. Iwakawa M, Ohno T, Imadome K, Nakawatari M, Ishikawa K, Sakai M, Katoh S, Ishikawa H, Tsujii H, Imai T. The radiation-induced cell-death signaling pathway is activated by concurrent use of cisplatin in sequential biopsy specimens from patients with cervical cancer. Cancer Biol Ther. 2007;6:905–11.
30. Han X, Zhou Z, Fei L, Sun H, Wang R, Chen Y, Chen H, Wang J, Tang H, Ge W, Zhou Y, Ye F, Jiang M, Wu J, Xiao Y, Jia X, Zhang T, Ma X, Zhang Q, Bai X, Lai S, Yu C, Zhu L, Lin R, Gao Y, Wang M, Wu Y, Zhang J, Zhan R, Zhu S, Hu H, Wang C, Chen M, Huang H, Liang T, Chen J, Wang W, Zhang D, Guo G. Construction of a human cell landscape at single-cell level. Nature. 2020;581:303–9.
31. Butler A, Hoffman P, Smibert P, Papalexi E, Satija R. Integrating single-cell transcriptomic data across different conditions, technologies, and species. Nature biotechnology. 2018;36:411–20.
32. Lall S, Sinha D, Bandyopadhyay S, Sengupta D. Structure-aware principal component analysis for single-cell rna-seq data. Journal of computational biology: a journal of computational molecular cell biology 2018.
33. Becht E, McInnes L, Healy J, Dutertre CA, Kwok IWH, Ng LG, Ginhoux F, Newell EW: Dimensionality reduction for visualizing single-cell data using umap. Nature biotechnology 2018.
34. Aran D, Looney AP, Liu L, Wu E, Fong V, Hsu A, Chak S, Naikawadi RP, Wolters PJ, Abate AR, Butte AJ, Bhattacharya M. Reference-based analysis of lung single-cell sequencing reveals a transitional profibrotic macrophage. Nature immunology. 2019;20:163–72.
35. Zhang X, Lan Y, Xu J, Quan F, Zhao E, Deng C, Luo T, Xu L, Liao G, Yan M, Ping Y, Li F, Shi A, Bai J, Zhao T, Li X, Xiao Y. Cellmarker: A manually curated resource of cell markers in human and mouse. Nucleic acids research. 2019;47:D721–8.
36. Franzen O, Gan LM, Bjorkegren JLM. Panglaodb: A web server for exploration of mouse and human single-cell rna sequencing data. Database: the journal of biological databases and curation 2019;2019.
37. Jemal A, Bray F, Center MM, Ferlay J, Ward E, Forman D. Global cancer statistics. Cancer J Clin. 2011;61:69–90.
38. Parkin DM, Bray F, Ferlay J, Pisani P. Estimating the world cancer burden: Globocan 2000. International journal of cancer. 2001;94:153–6.
39. Scatchard K, Forrest JL, Flubacher M, Cornes P, Williams C. Chemotherapy for metastatic and recurrent cervical cancer. Cochrane Database Syst Rev. 2012;10:CD006469.
40. Shrivastava S, Mahantshetty U, Engineer R, Chopra S, Hawaldar R, Hande V, Kerkar RA, Maheshwari A, Shylasree TS, Ghosh J, Bajpai J, Gurram L, Gulia S, Gupta S. Gynecologic Disease Management G:

Cisplatin chemoradiotherapy vs radiotherapy in figo stage iiib squamous cell carcinoma of the uterine cervix: A randomized clinical trial. JAMA oncology. 2018;4:506–13.

41. Schiffman M, Castle PE, Jeronimo J, Rodriguez AC, Wacholder S. Human papillomavirus and cervical cancer. Lancet. 2007;370:890–907.
42. Bosch FX, Burchell AN, Schiffman M, Giuliano AR, de Sanjose S, Bruni L, Tortolero-Luna G, Kjaer SK, Munoz N. Epidemiology and natural history of human papillomavirus infections and type-specific implications in cervical neoplasia. Vaccine. 2008;26(Suppl 10):K1–16.
43. Eke I, Cordes N. Focal adhesion signaling and therapy resistance in cancer. Sem Cancer Biol. 2015;31:65–75.
44. Cimbora-Zovko T, Ambriovic-Ristov A, Loncarek J, Osmak M. Altered cell-cell adhesion in cisplatin-resistant human carcinoma cells: A link between beta-catenin/plakoglobin ratio and cisplatin resistance. Eur J Pharmacol. 2007;558:27–36.
45. White DE, Rayment JH, Muller WJ. Addressing the role of cell adhesion in tumor cell dormancy. Cell cycle. 2006;5:1756–9.
46. Kesh K, Gupta VK, Durden B, Garrido V, Mateo-Victoriano B, Lavania SP, Banerjee S. Therapy resistance, cancer stem cells and ecm in cancer: The matrix reloaded. Cancers 2020;12.

Tables

Due to technical limitations, table 1 is only available as a download in the Supplemental Files section.

Figures

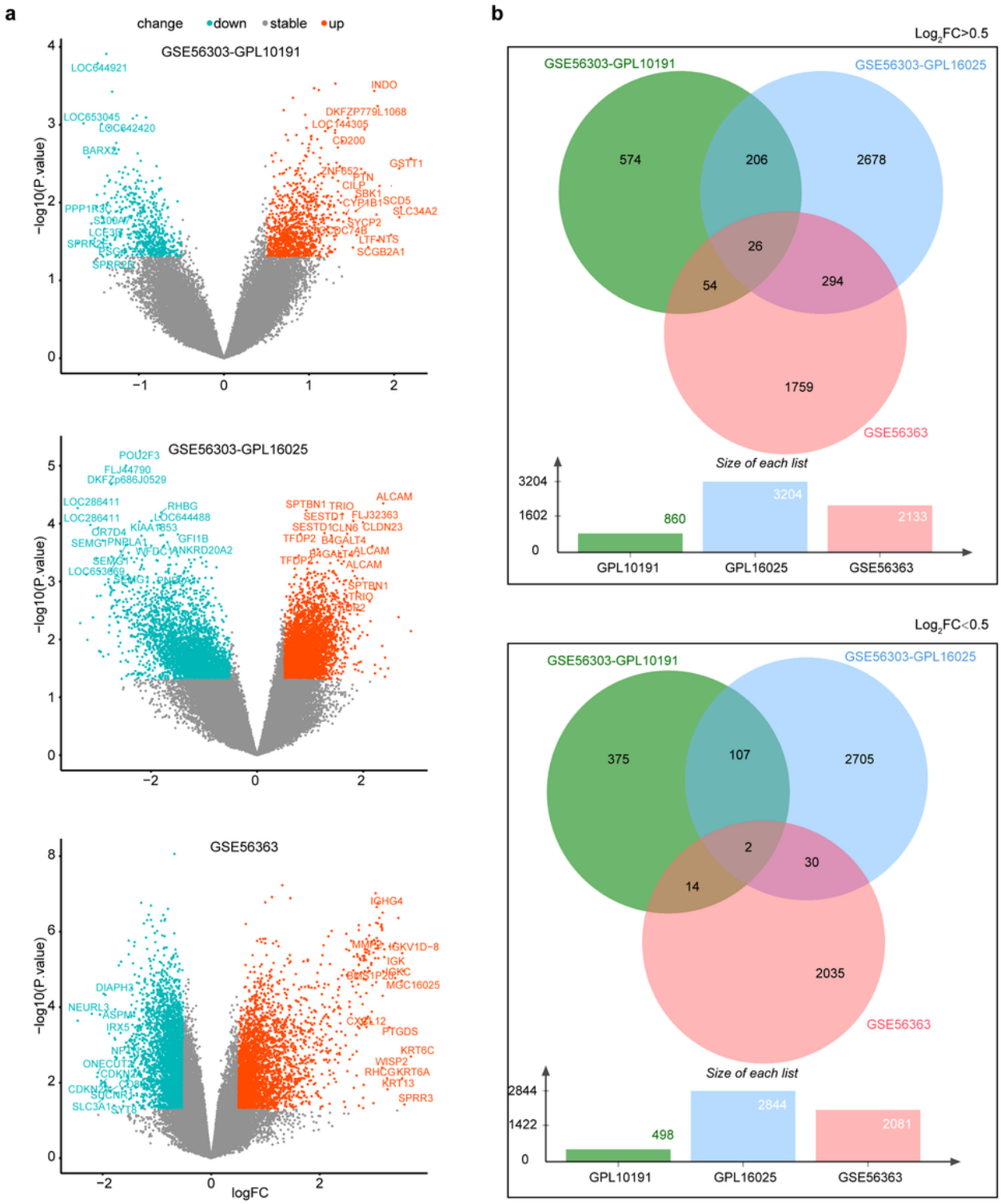

Figure 1

Identification of DEGs in LACC microarray datasets. (a) Volcano plots were used to show the overall distribution of DEGs between responders and non-responders, red represents up-regulated genes, light blue represents down-regulated genes. (b) Venn diagram of the EDGs in the 3 datasets. A total of 580 up-regulated DEGs and 153 down-regulated DEGs were screened out.

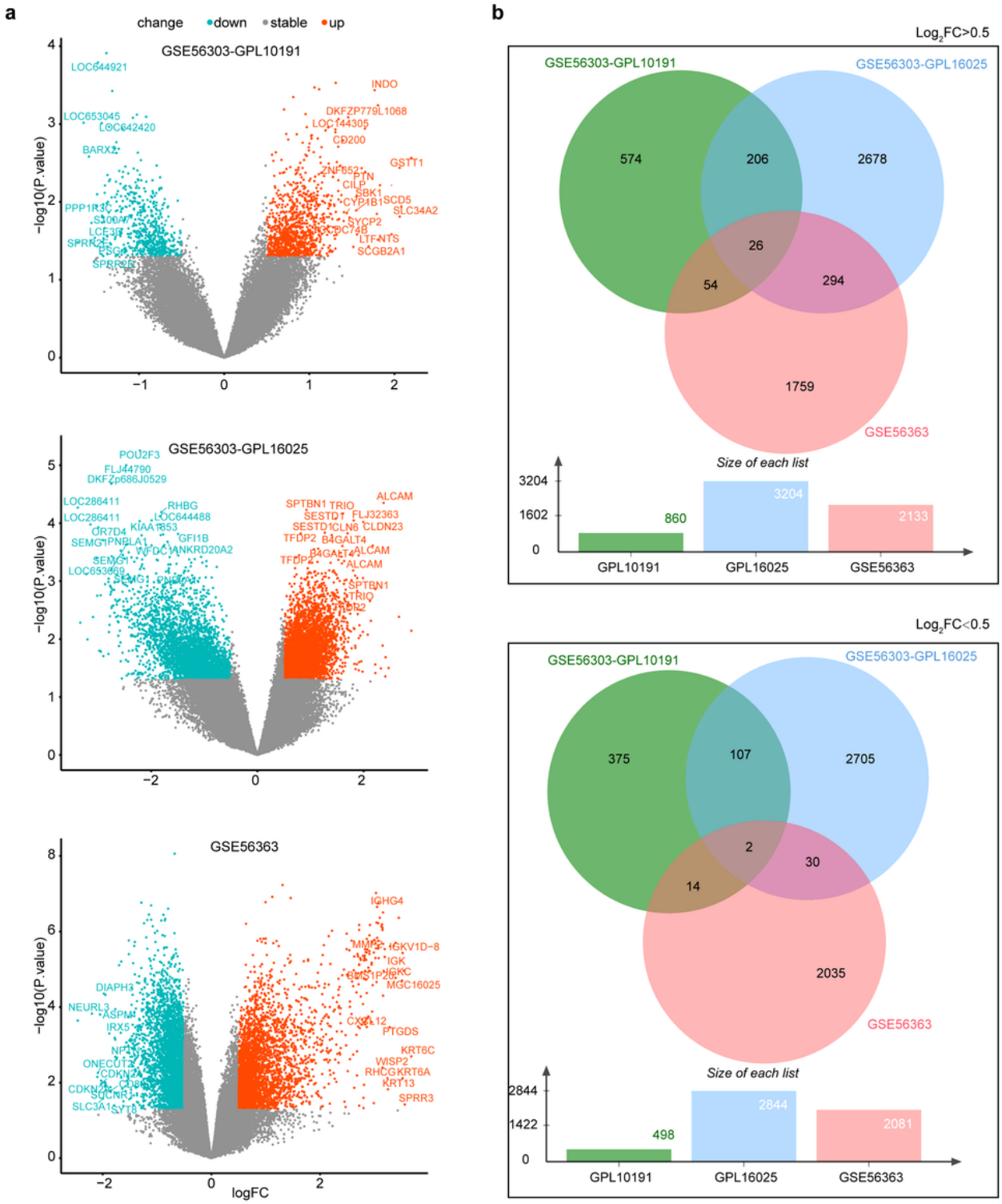

Figure 1

Identification of DEGs in LACC microarray datasets. (a) Volcano plots were used to show the overall distribution of DEGs between responders and non-responders, red represents up-regulated genes, light blue represents down-regulated genes. (b) Venn diagram of the EDGs in the 3 datasets. A total of 580 up-regulated DEGs and 153 down-regulated DEGs were screened out.

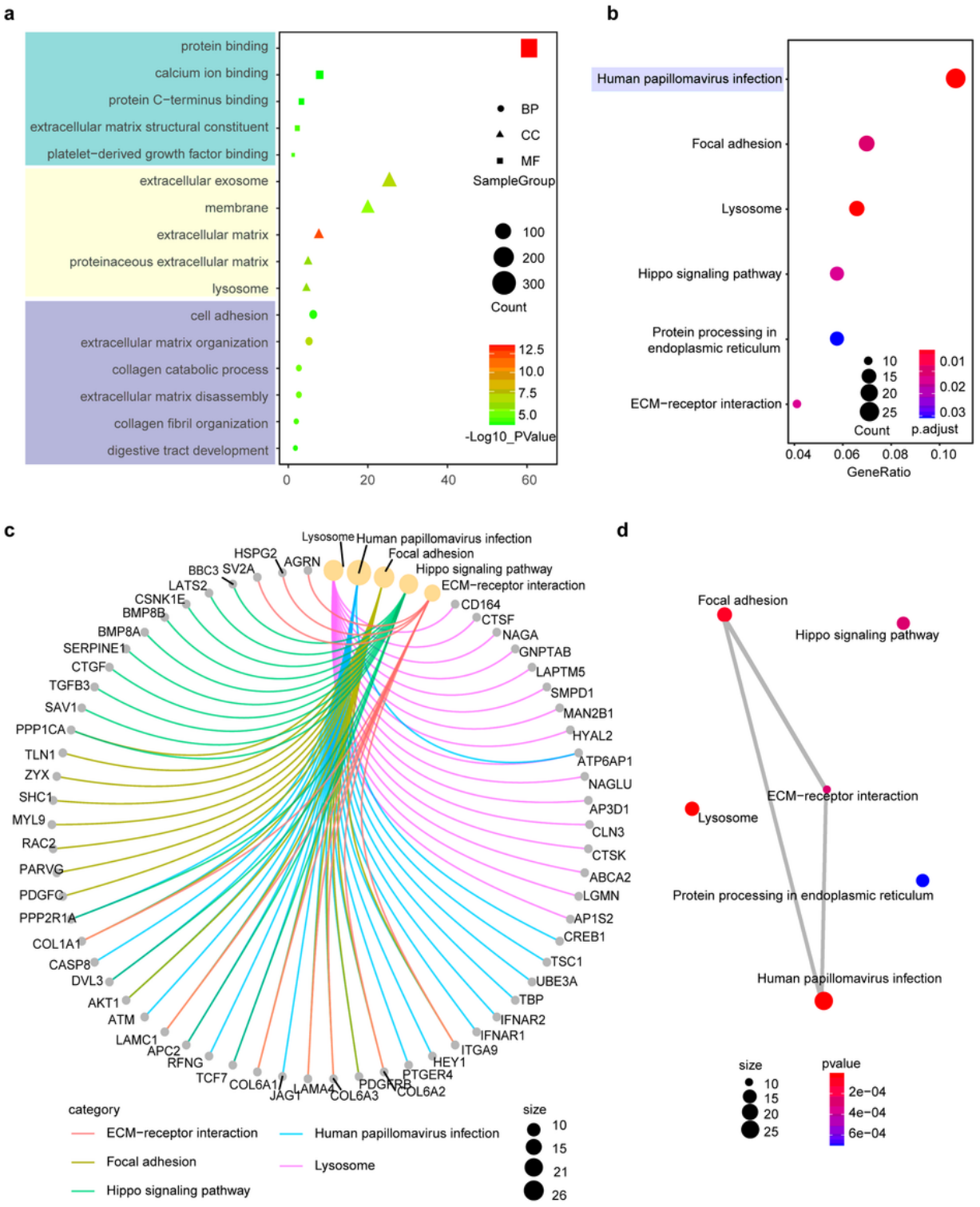

Figure 2

GO and KEGG signaling pathways analysis of the DEGs in LACC. (a) The BP/MF/CC of GO analysis of 580 up-regulated DEGs. (b) Scatter plot of KEGG pathway enrichment statistics. (c) cnetplot of KEGG signal pathway shown the “pathway-gene” network. (d) emapplot of KEGG signal pathway shown the “pathway-pathway” network.

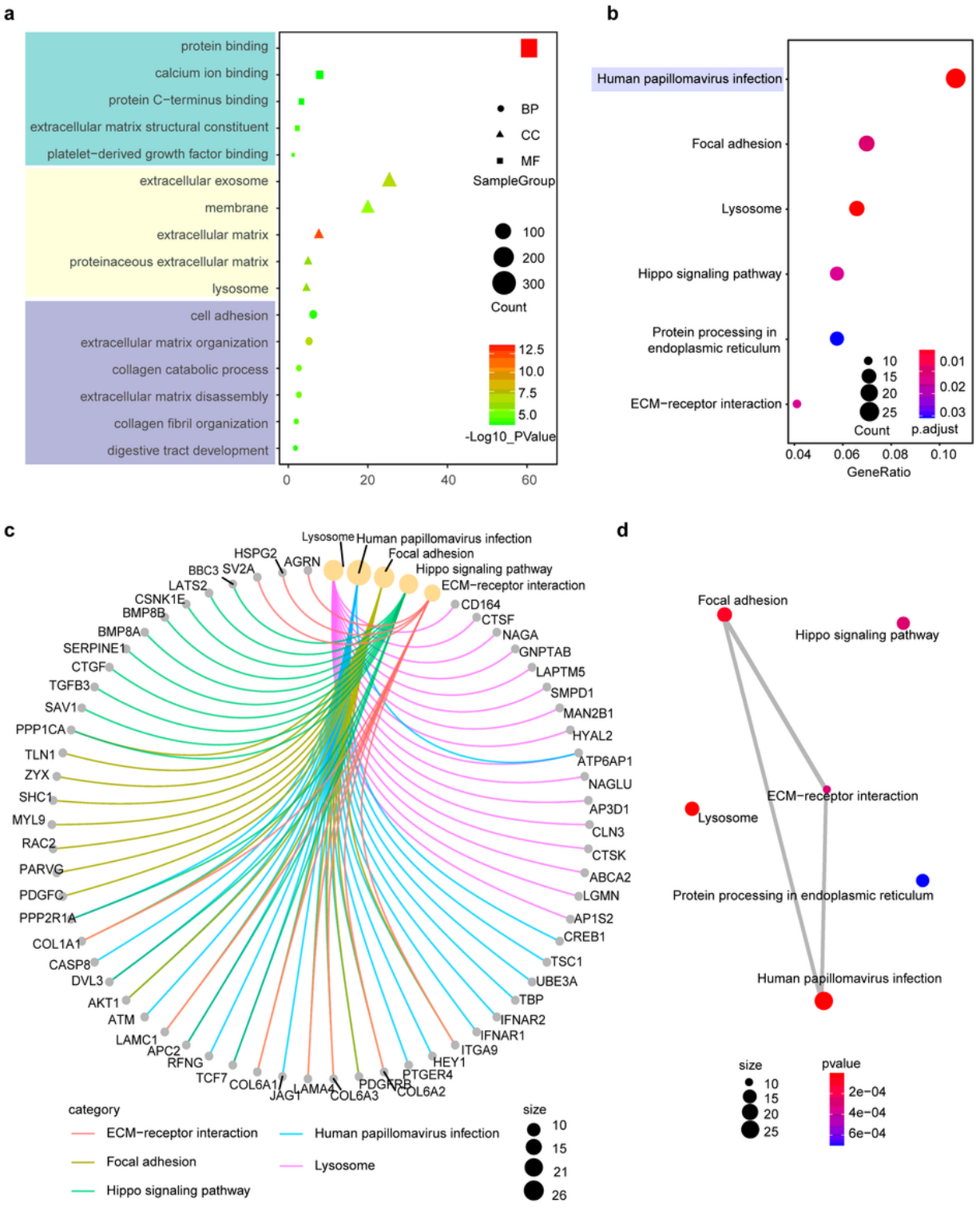

Figure 2

GO and KEGG signaling pathways analysis of the DEGs in LACC. (a) The BP/MF/CC of GO analysis of 580 up-regulated DEGs. (b) Scatter plot of KEGG pathway enrichment statistics. (c) cnetplot of KEGG signal pathway shown the “pathway-gene” network. (d) emapplot of KEGG signal pathway shown the “pathway-pathway” network.

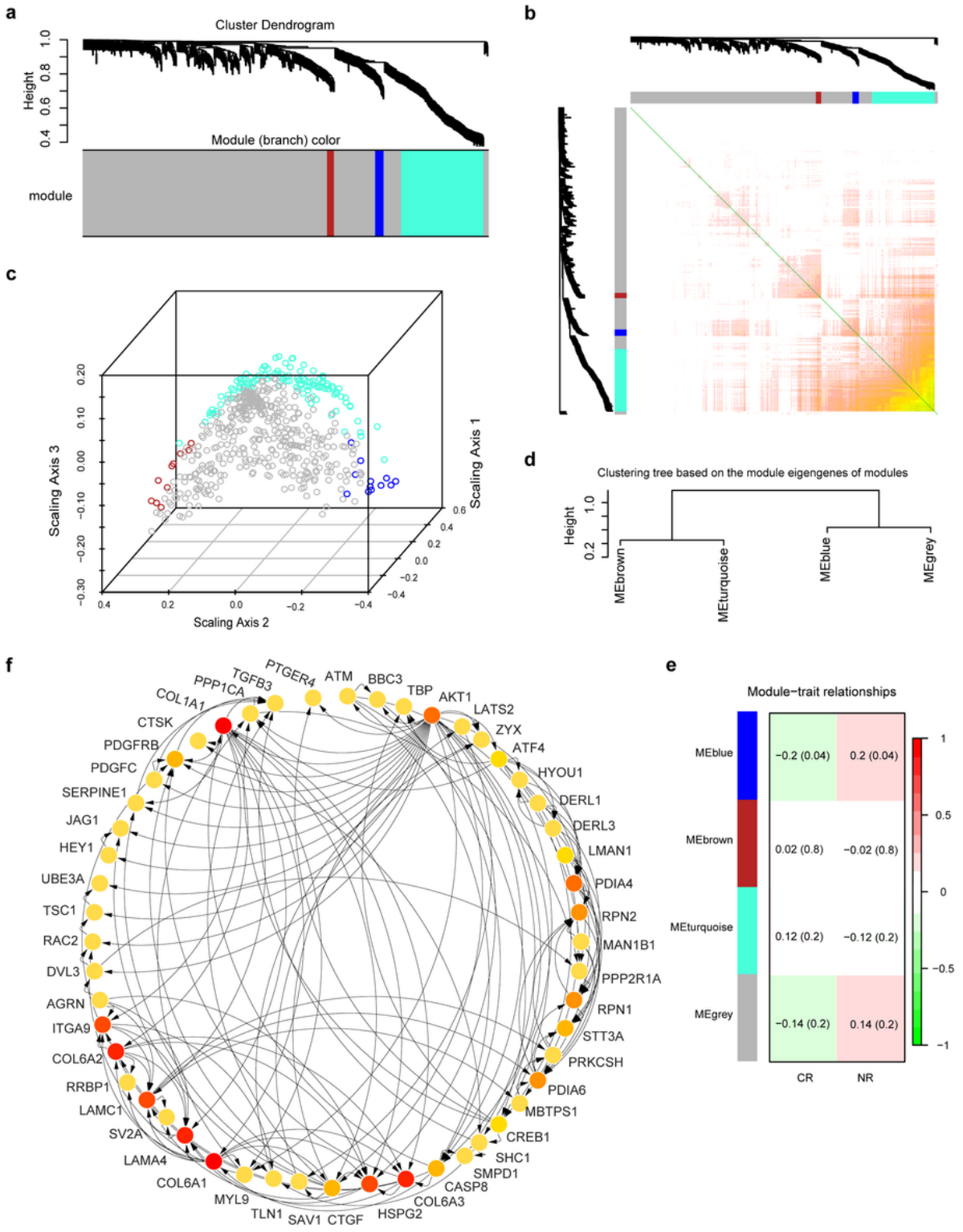

Figure 3

Identification of genes associated with clinical features and hub genes identification. (a) Gene dendrogram obtained by average linkage hierarchical clustering. A total of 4 modules were identified. (b) Heatmap plot of topological overlap in the gene network. Each row and column corresponds to a gene, light color denotes low topological overlap, and progressively darker denotes higher topological overlap. (c) Results of multidimensional scaling. (d) Relationships among modules was summarized by a

hierarchical clustering dendrogram of their eigengenes. (e) Relationships of consensus module eignegenes and clinical features. Numbers in the table report the correlations of the corresponding module eigengenes and treatment effect, with the p values printed in parentheses. (f) There were a total of 52 DEGs in the PPI network complex. The nodes meant proteins; the edges meant the interaction of proteins. Hub genes screened by MCC algorithms from cytoHubba, the darker the color, the bigger the degrees.

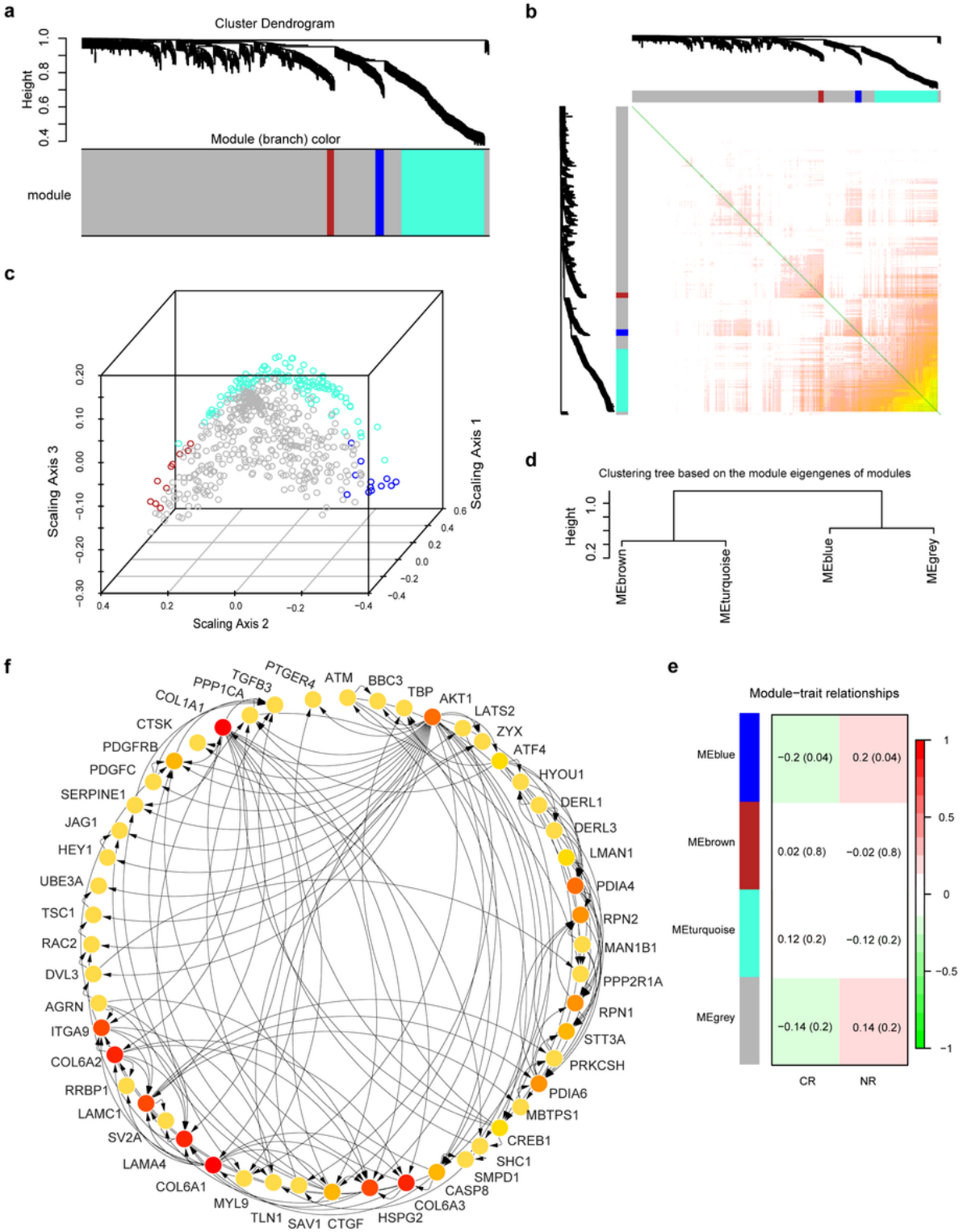

Figure 3

Identification of genes associated with clinical features and hub genes identification. (a) Gene dendrogram obtained by average linkage hierarchical clustering. A total of 4 modules were identified. (b) Heatmap plot of topological overlap in the gene network. Each row and column corresponds to a gene, light color denotes low topological overlap, and progressively darker denotes higher topological overlap. (c) Results of multidimensional scaling. (d) Relationships among modules was summarized by a hierarchical clustering dendrogram of their eigengenes. (e) Relationships of consensus module eignegenes and clinical features. Numbers in the table report the correlations of the corresponding module eigengenes and treatment effect, with the p values printed in parentheses. (f) There were a total of 52 DEGs in the PPI network complex. The nodes meant proteins; the edges meant the interaction of proteins. Hub genes screened by MCC algorithms from cytoHubba, the darker the color, the bigger the degrees.

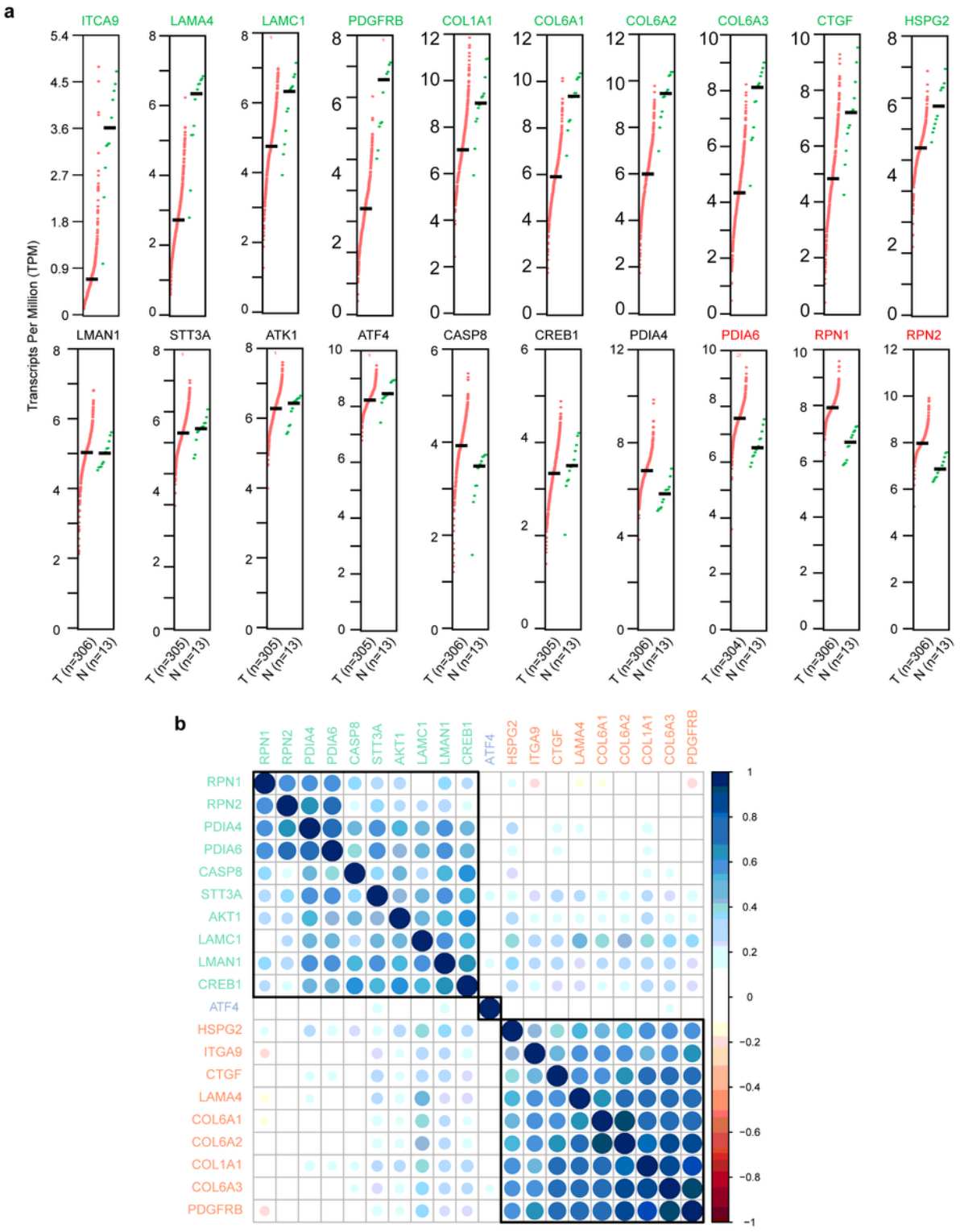

Figure 4

Expression analysis of 20 hub genes. (a) Comparison of expression levels between cervical cancer patients and normal controls. Red represents the cancer group, and the green represents the normal group. (b) The heat map shows the co-expression relationship of hub genes, red represents negative correlation, blue represents positive correlation, and the larger the circle is, the smaller the P-value is.

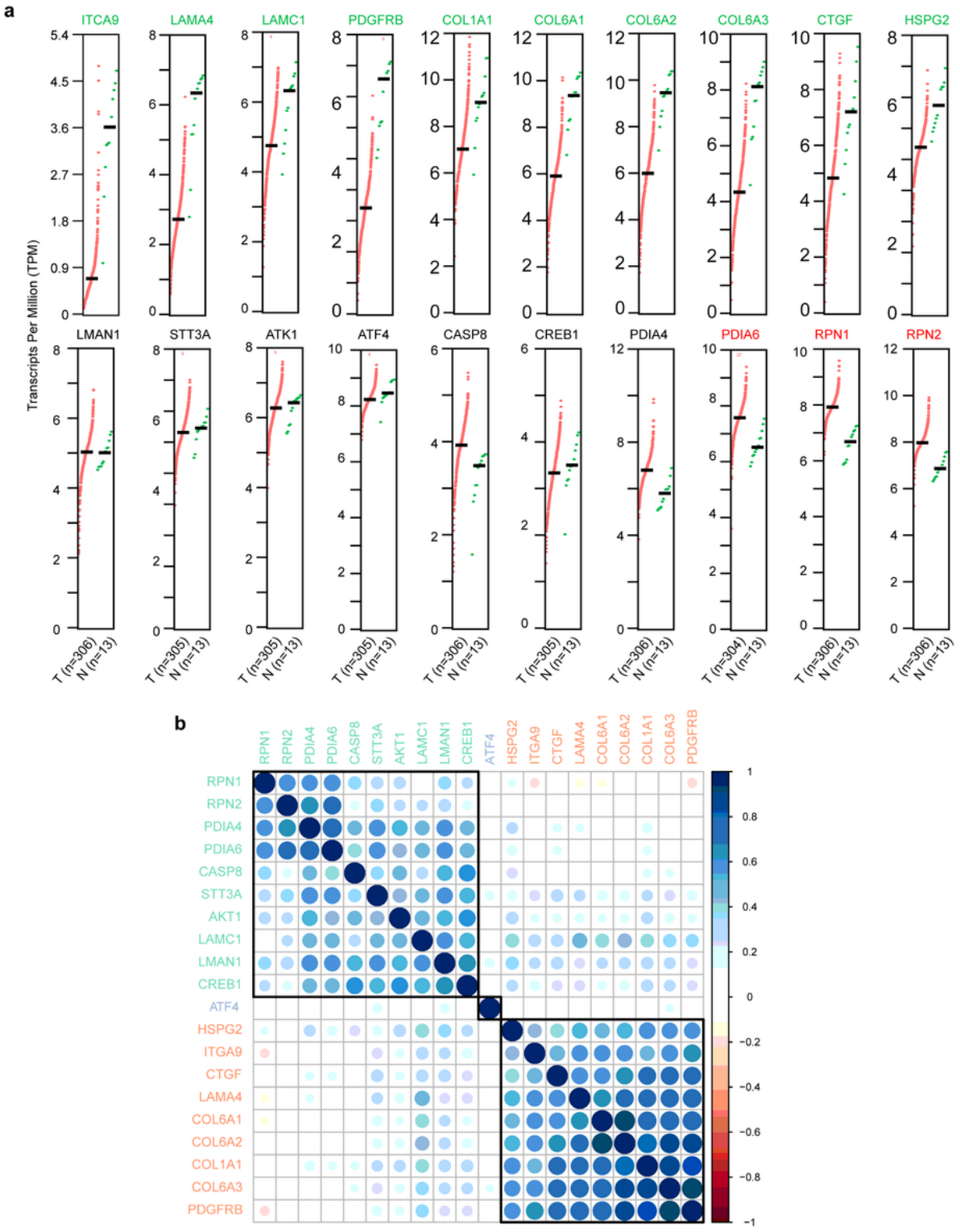

Figure 4

Expression analysis of 20 hub genes. (a) Comparison of expression levels between cervical cancer patients and normal controls. Red represents the cancer group, and the green represents the normal group. (b) The heat map shows the co-expression relationship of hub genes, red represents negative correlation, blue represents positive correlation, and the larger the circle is, the smaller the P-value is.

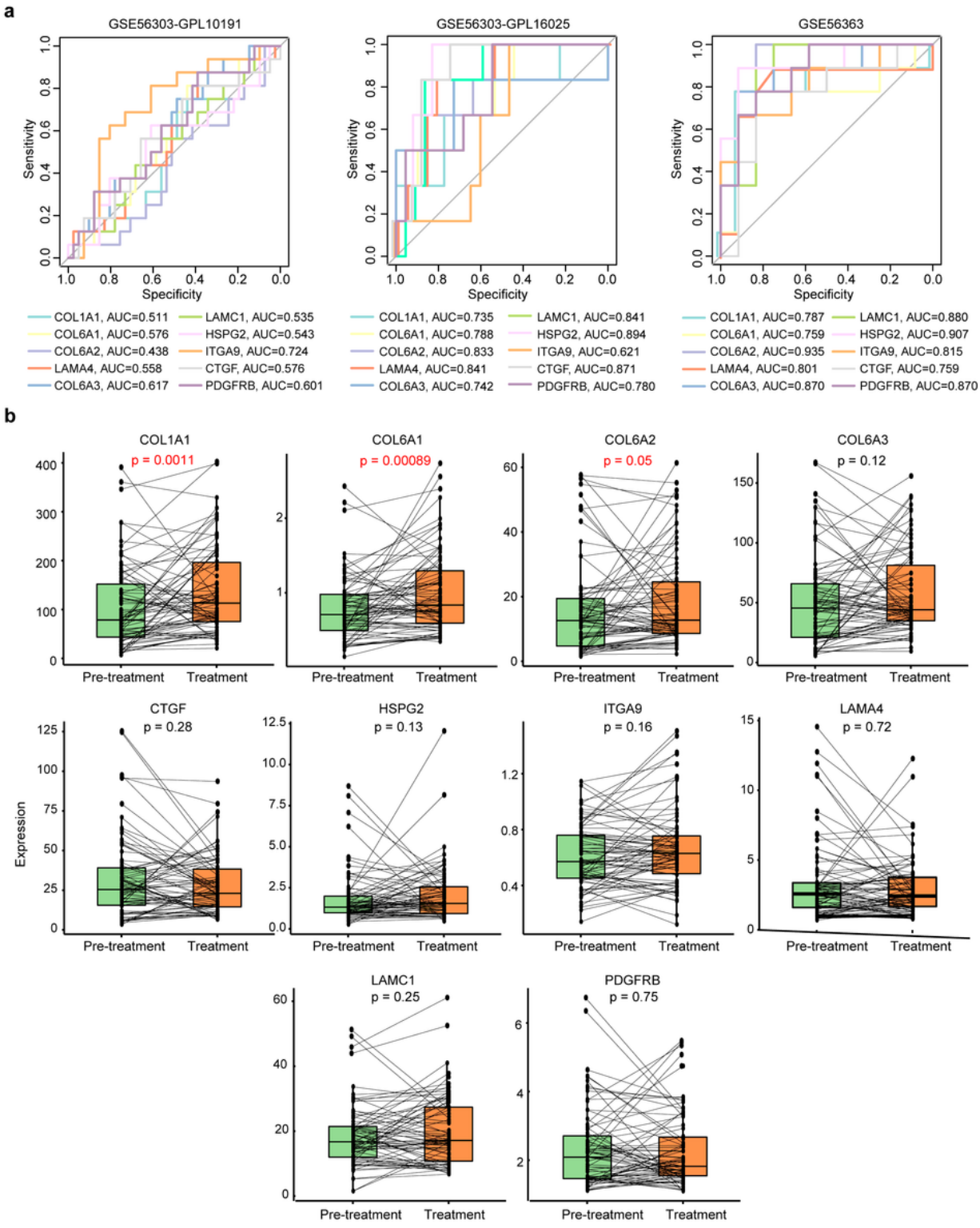

Figure 5

Further analysis of 10 down-regulated genes in cancer. (a) ROC curve showed the accuracy of gene expression in predicting the results of chemoradiotherapy. Different colors indicate different genes. (AUC, the area under the curve; ROC, receiver operating characteristic curve) (b) Changes of expression levels of 10 hub genes before and after chemoradiotherapy. Green indicates the level of gene expression before

radiotherapy or chemoradiotherapy; Red indicates the level of gene expression after radiotherapy or chemoradiotherapy. (Paired T-test, P <0.05 was statistically significant)

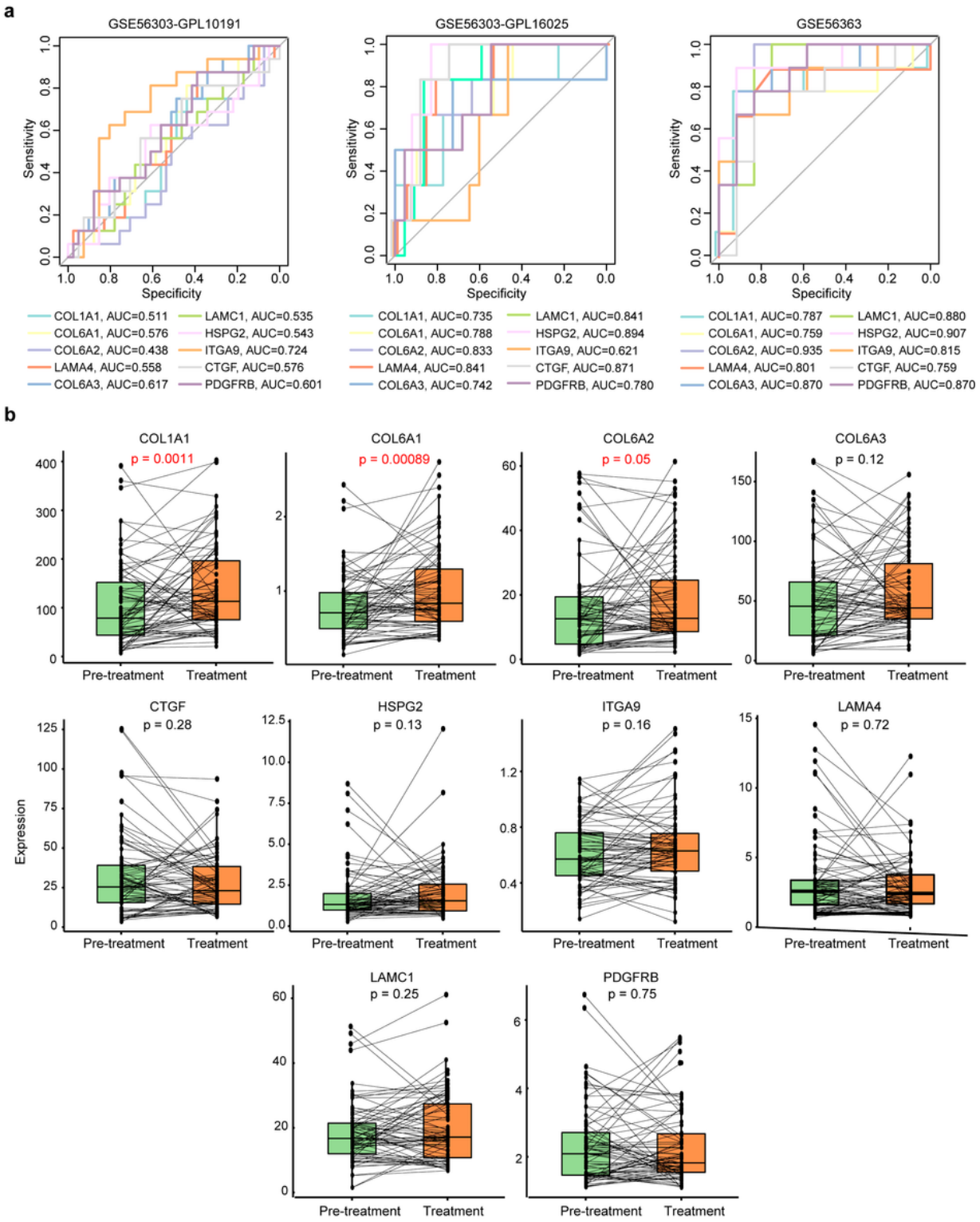

Figure 5

Further analysis of 10 down-regulated genes in cancer. (a) ROC curve showed the accuracy of gene expression in predicting the results of chemoradiotherapy. Different colors indicate different genes. (AUC, the area under the curve; ROC, receiver operating characteristic curve) (b) Changes of expression levels of

10 hub genes before and after chemoradiotherapy. Green indicates the level of gene expression before radiotherapy or chemoradiotherapy; Red indicates the level of gene expression after radiotherapy or chemoradiotherapy. (Paired T-test, P <0.05 was statistically significant)

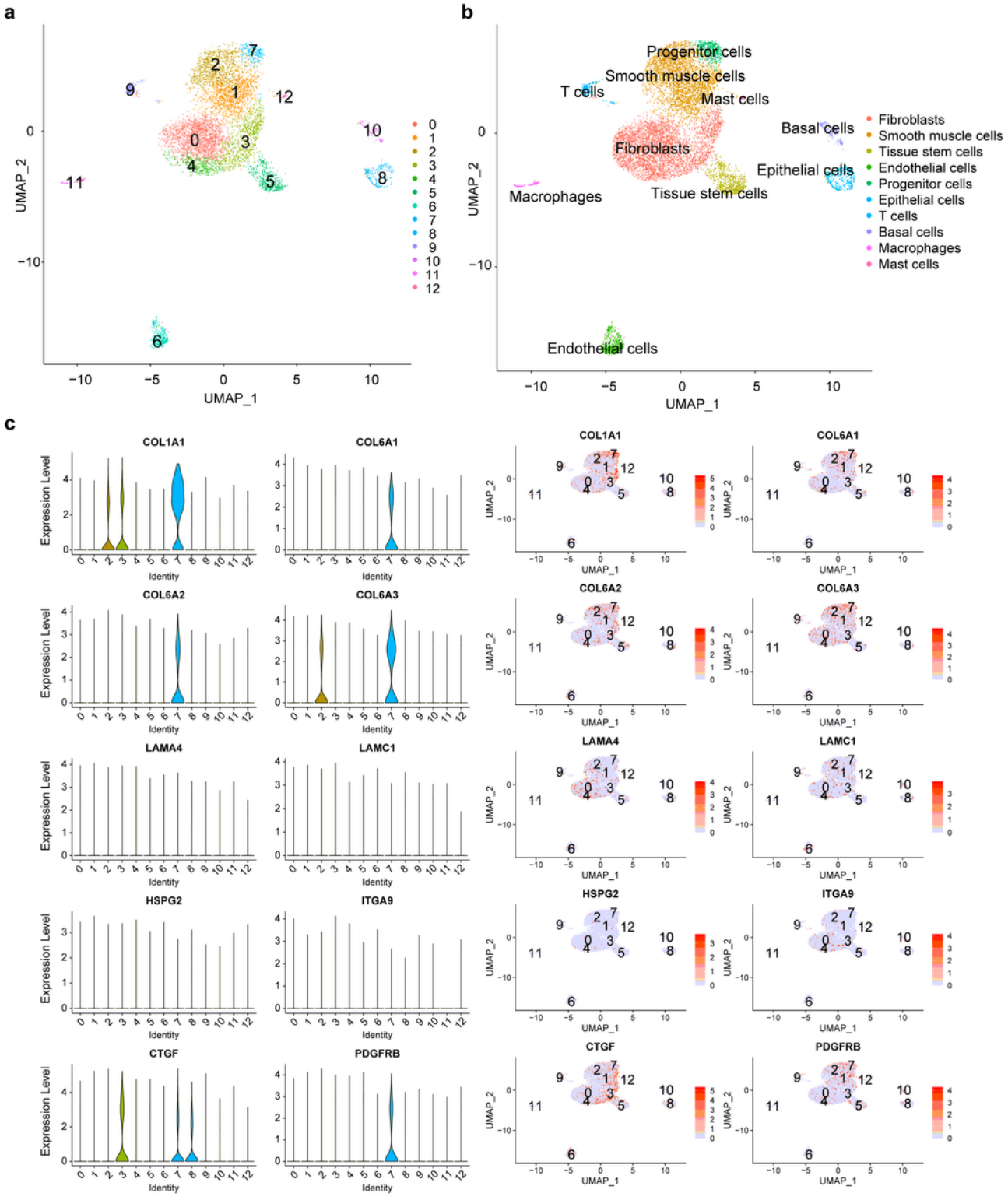

Figure 6

The cell types of cervical tissue and the expression level of 10 hub genes in cervical tissue cells. (a) Identification of 12 cell clusters based on single-cell RNA sequence data. The UMAP algorithm was

applied for dimensionality reduction with the 20 PCs. (b) All 12 clusters of cells in the cervix were annotated by singleR, CellMarker, and PanglaoDB according to the composition of the marker genes. (c) Violin diagrams and UMAP diagrams showed the expression level of genes in 12 clusters.

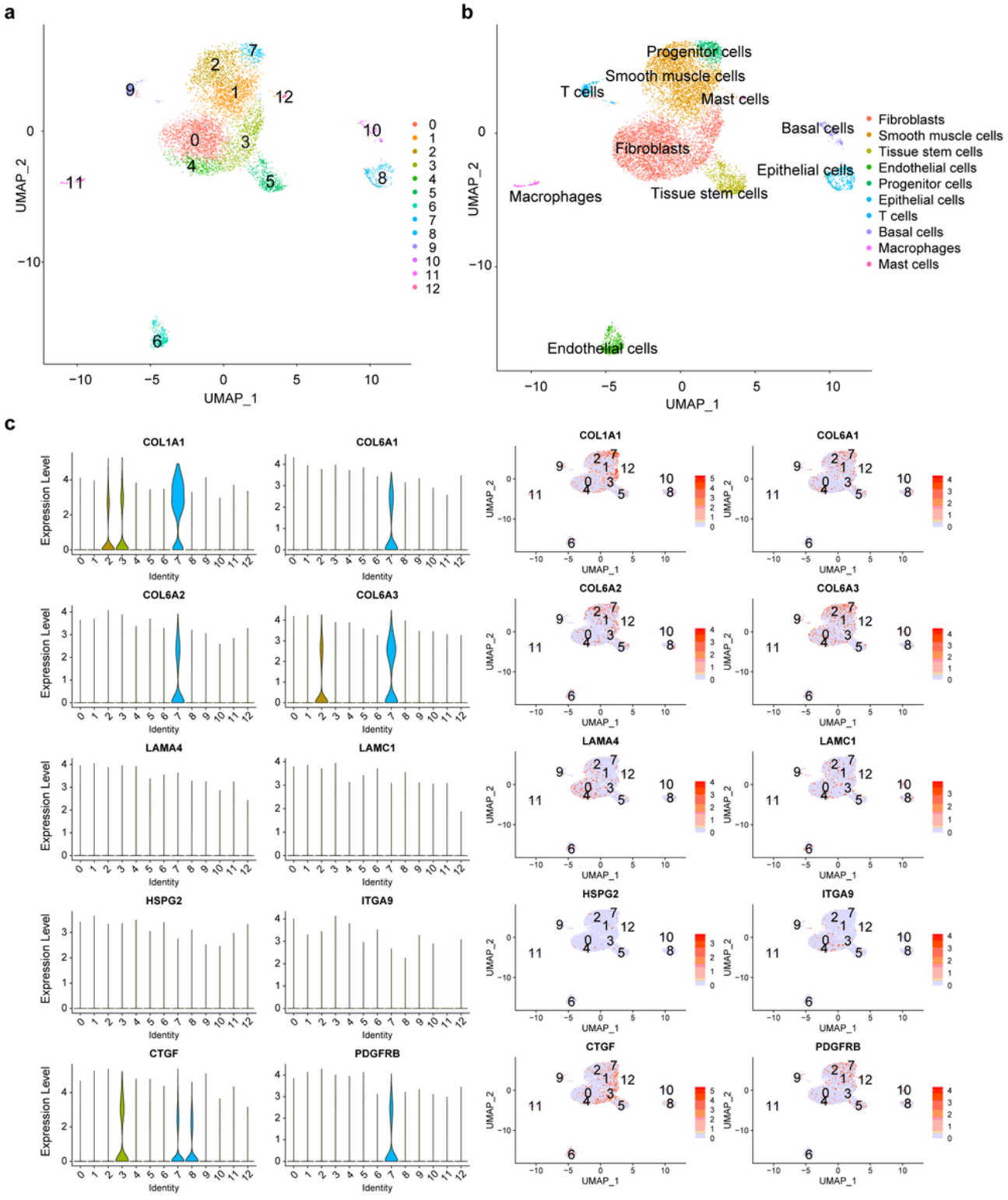

Figure 6

The cell types of cervical tissue and the expression level of 10 hub genes in cervical tissue cells. (a) Identification of 12 cell clusters based on single-cell RNA sequence data. The UMAP algorithm was

applied for dimensionality reduction with the 20 PCs. (b) All 12 clusters of cells in the cervix were annotated by singleR, CellMarker, and PanglaoDB according to the composition of the marker genes. (c) Violin diagrams and UMAP diagrams showed the expression level of genes in 12 clusters.

Supplementary Files

This is a list of supplementary files associated with this preprint. Click to download.

- Table1.xlsx
- Table1.xlsx
- SupplementaryTable2.xlsx
- SupplementaryTable2.xlsx
- SupplementaryTable3.xlsx
- SupplementaryTable3.xlsx
- SupplementaryTable4.xlsx
- SupplementaryTable4.xlsx
- SupplementaryTable5.xlsx
- SupplementaryTable5.xlsx
- SupplementaryFigure1.pdf
- SupplementaryFigure1.pdf
- SupplementaryFigure2.pdf
- SupplementaryFigure2.pdf
- SupplementaryFigure3.pdf
- SupplementaryFigure3.pdf